

Deep Learning for Optimal Phase-Shift and Beamforming Based on Individual and Cascaded Channels Estimation in the RIS-MIMO System

walaa hussein¹, Nor Noordin², Mohd A.Rasid², Alyani Ismail², kamil Kareem², and Aymen Flah³

¹Iraq University College

²Universiti Putra Malaysia

³University of Gabes

March 17, 2024

Abstract

Reconfigurable Intelligent Surfaces (RIS) represent an advanced technology reshaping wireless communication networks. Through intelligent configuration of wireless propagation environments using both cost-effective passive and active elements, RIS has the potential to bring about considerable performance improvements. In RIS-MIMO systems, precise control of passive RIS elements is crucial in optimizing reflected signal phases. This control necessitates intricate algorithms, given that inaccurate phase optimization can result in suboptimal signal focus and decreased data transmission accuracy. Obtaining accurate channel state information (CSI) is vital for achieving optimal phase control and high data rates; however, estimating channels between the transmitter, RIS, and receiver poses challenges. This paper investigates deep learning methodologies for channel estimation, explicitly addressing the distinctive challenges associated with phase shifts and beamforming. We present tailored deep-learning algorithms for each estimation technique, showcasing notable improvements in estimation accuracy, computational efficiency, and adaptability in dynamic environments.

Hosted file

IET Submission Template.docx available at <https://authorea.com/users/713939/articles/728518-deep-learning-for-optimal-phase-shift-and-beamforming-based-on-individual-and-cascaded-channels-estimation-in-the-ris-mimo-system>

Deep Learning for Optimal Phase-Shift and Beamforming Based on Individual and Cascaded Channels Estimation in the RIS-MIMO System

Wala'a Hussein^{1,2,3*}, Nor Kamariah Noordin^{1,2,*}, Kamil Audah^{1,2,3}, Mohd Fadlee A.Rasid^{1,2}, Alyani Binti Ismail^{1,2}, Aymen Flah^{4,5}

¹ Department of Computer and Communications Systems Engineering, Universiti Putra Malaysia, 43400 UPM Serdang Selangor Darul Ehsan, Malaysia.

² Wireless and Photonic Networks Research Centre of Excellence (WiPNET), Faculty of Engineering and Technology, Universiti Putra Malaysia (UPM), Serdang, Selangor Darul Ehsan 43400, Malaysia.

³ Department of Computer Technology Engineering, Faculty of Engineering, Iraq University College, Basra, Iraq

⁴ Processes, Energy, Environment and Electrical Systems, National Engineering School of Gabes, University of Gabes, Gabes 6072, Tunisia

⁵ The Private Higher School of Applied Sciences and Technology of Gabes, University of Gabes, Gabes, Tunisia

* walaahussein613@gmail.com, nknordin@upm.edu.my,

Abstract: Reconfigurable Intelligent Surfaces (RIS) represent an advanced technology reshaping wireless communication networks. Through intelligent configuration of wireless propagation environments using both cost-effective passive and active elements, RIS has the potential to bring about considerable performance improvements. In RIS-MIMO systems, precise control of passive RIS elements is crucial in optimizing reflected signal phases. This control necessitates intricate algorithms, given that inaccurate phase optimization can result in suboptimal signal focus and decreased data transmission accuracy. Obtaining accurate channel state information (CSI) is vital for achieving optimal phase control and high data rates; however, estimating channels between the transmitter, RIS, and receiver poses challenges. This paper investigates deep learning methodologies for channel estimation, explicitly addressing the distinctive challenges associated with phase shifts and beamforming. We present tailored deep-learning algorithms for each estimation technique, showcasing notable improvements in estimation accuracy, computational efficiency, and adaptability in dynamic environments.

1. Introduction

Considerable interest has been devoted to the reconfigurable intelligent surface (RIS) [1]. Secure communications [5], uncrewed aerial vehicles [2], and energy efficiency [4] are some of its many uses. Figure 1 is an example of a RIS-assisted MIMO network. When the source node S contains many antennas, optimizing the phase shift at the RIS and the beamforming at the source simultaneously is necessary. This process requires the channel state information (CSI) of all connections. Individual channels are used for $S \rightarrow \text{RIS}$ and $\text{RIS} \rightarrow D$ linkages, whereas cascaded channels are implemented for end-to-end $S \rightarrow \text{RIS} \rightarrow D$ links.

It is challenging to get individual $S \rightarrow \text{RIS}$ and $\text{RIS} \rightarrow D$ channel estimations (e.g., [6]). The individual $S \rightarrow \text{RIS}$ and $\text{RIS} \rightarrow D$ channels may be approximated with a degree of uncertainty in [7]. The Tensor modeling technique was implemented in [8] to estimate individual channels in the MIMO RIS network. The researchers used an iterative process [9] to calculate the individual channels. On the other hand, the estimation of the cascaded $S \text{ RIS } D$ channels is more straightforward.

In [10] and [11], the concept of cascaded channel estimation is recommended for the SISO scenario (where a single antenna is employed at both the source and destination nodes), double RIS panels, and the MISO RIS-assisted network, respectively. As indicated in [12], deep learning techniques were employed to estimate cascaded channels in

MISO OFDM. Estimating cascaded channels often presents challenges, particularly in clearly expressing the end-to-end channel capacity, mainly when many antennas are utilized at both the source and destination nodes. This leads to the implementation of combined phase shift and beamforming. On the contrary, though estimating individual channels poses difficulties, integrating phase shift and beamforming is regarded as a more conventional approach. The proposal encompasses joint phase shift and beamforming, involving both cascaded and separate channels.

For example, [8] and [9] determined the joint optimization of beamforming and phase adjustment for the RIS-assisted MIMO network by relying on individual channel estimates. The optimization of phase adjustment in the cascaded channel of the SISO OFDM RIS network, where beamforming at the source node is unnecessary, was achieved in [13]. The authors then investigated RIS-assisted MIMO beamforming through the cascaded channel in [14]. In this method, the process of beamforming and phase correction is repeated. Furthermore, the phases of the RIS are iteratively optimized. At any given moment, only the phase of a single element is optimized, while the phases of the other components remain constant.

The mathematical optimization methods mentioned above require significant online computing resources. Employing iterative optimization techniques for beamforming and phase shift in the MIMO RIS network is crucial, adding complexity to implementation and placing a

more significant burden on online computations due to convergence issues. Moreover, optimizations are frequently carried out using simplified models, assuming constant amplitude gains across different phase shifts. When this assumption is not satisfied [15], [16], the optimization process becomes more intricate.

Recent advancements in machine learning offer attractive alternatives for the phase transition in RIS (e.g., [17], [18], [19], [20], [21]). However, reinforcement learning (RL) and related algorithms are not optimal for most RIS systems. This is because RL requires implementation with correlated data samples, where state changes occur due to actions. In contrast, this characteristic does not align with the RIS phase shift issue, as elaborated in Section III. Achieving RL convergence would be highly challenging, especially in cases involving a significant number of components in an RIS, as will be demonstrated in simulations. This letter introduces a novel deep neural network model comprising two separate networks. Unlike RL, the proposed double deep neural network performs effectively in scenarios with numerous RIS components.

1.1. state of the art of CSI estimation in RIS-MIMO systems

The last few years have witnessed a substantial evolution in wireless communication systems, with a notable emphasis on integrating deep learning techniques. Researchers have increasingly explored the application of convolutional neural networks (CNNs) and recurrent neural networks (RNNs) to address complex challenges in channel estimation, adaptive modulation, and beamforming [1]. In parallel, Reconfigurable Intelligent Surface (RIS) technology has gained significant attention for its potential to revolutionize wireless communication. Recent works have focused on seamlessly integrating RIS into multiple input and multiple output (MIMO) systems to enhance overall communication performance. Noteworthy advancements in channel estimation methodologies, particularly those considering individual and cascaded channels, have been a focal point of research [4]. Optimal phase-shift control and beamforming strategies have become pivotal components in RIS-enabled communication systems. Recent studies underscore the critical role of intelligent algorithms, including deep learning models, in dynamically optimizing phase shifts and beamforming parameters to achieve superior signal quality and system performance [9]. Against this backdrop, the paper contributes to the current discourse by proposing a novel approach that harnesses deep learning techniques for optimizing phase-shift and beamforming in the context of individual and cascaded channel estimation within RIS-MIMO systems. This aligns with the prevailing trend of leveraging artificial intelligence to overcome the challenges presented by dynamic and complex wireless environments [10].

1.2. Motivation

Reconfigurable Intelligent Surface (RIS) is required and considered a trending technology in wireless communication because it can enhance signal propagation, increase system capacity, and improve communication performance by manipulating signals using passive and active components. RIS offers adaptability, low complexity, and energy efficiency, making it a promising technology for

future wireless networks. RIS thus holds great potential for improving the performance of wireless communication systems, particularly in the context of 5G and beyond. Channel estimation in RIS-MIMO is motivated by the need to deal effectively with the challenges of fast-changing signal conditions. Fast fading channels, characterized by rapid signal strength and phase fluctuations, require constant updates of channel state information (CSI) to ensure adaptability. The use of image-based representations for channel modeling underscores the importance of obtaining clear and precise images, free from interference or noise, to accurately capture the state of the channel.

Additionally, actively managing the phase shift by RIS elements is crucial for optimizing how signals are reflected, especially in the face of fast-fading effects. This optimization enhances the system's ability to adjust dynamically, ensuring reliable communication. In essence, the motivation is centered around staying responsive to dynamic conditions, improving the quality of image data, and fine-tuning control over phase shifts for efficient signal transmission in RIS-MIMO systems.

1.3. Background and related work:

Obtaining Channel State Information (CSI) poses a significant challenge in deploying RIS-assisted systems. CSI for the pertinent wireless links is essential for the joint design of active beamforming at the transceiver and passive beamforming (reflection coefficient matrix) at the RIS. This section briefly overviews the critical challenges of channel estimation in RIS-assisted systems. A summary of the latest techniques for channel estimation is presented, along with a detailed examination of the advantages, limitations, and applicable scenarios for each method.

Reconfigurable Intelligent Surfaces (RIS) have brought a groundbreaking approach in the wireless domain, reshaping the environment to enhance signal propagation [23]. The integration of RIS with MIMO systems has enabled more advanced communication pathways, thereby improving the quality and reliability of transmissions. Dimitriou and Patel (2023) comprehensively analyzed the possibilities and challenges of these integrated systems, underscoring the importance of improved channel estimation techniques [24]. Channel estimation, a crucial element in ensuring effective communication, has witnessed the development of numerous techniques over the years. While deterministic methods were once predominant, they are now considered insufficient for addressing the complexities introduced by RIS-MIMO systems [25]. Sanghvi and Bhat's (2021) research demonstrated an advanced deterministic model for individual channel behaviors but encountered difficulties in dynamic scenarios [26].

Integrating artificial intelligence, specifically deep learning, into wireless communication offers a promising avenue for addressing these challenges. In 2023, Anand and Prakash's groundbreaking research utilized conventional neural networks for cascaded channel estimation in RIS-MIMO systems, revealing limitations in high-mobility environments [27]. Building upon this, Lui and Tan (2022) further advanced the research by emphasizing convolutional neural networks (CNNs) to capture time-frequency patterns. Their work led to significant enhancements, particularly in scenarios marked by swift temporal variations [28].

Although progress has been achieved in incorporating deep learning for channel estimation in RIS-MIMO configurations, there remains a notable gap in offering a comprehensive solution that addresses both cascaded and individual channels. Additionally, with the growing discussion on 6G, the demand for a robust, adaptive, and real-time channel estimation technique becomes crucial. Reconfigurable Intelligent Surface (RIS) assisted MIMO systems have undergone substantial advancements from 2019 to the present. Two main focal points have been optimizing phase shifts and predicting data rates, each with distinct approaches tailored for cascaded and individual channel scenarios.

Optimizing phase shifts has emerged as a pivotal research focus in cascaded channels. Smith et al. (2021) pioneered this field with their gradient-based approach, leveraging channel state information to improve received signal strength [32]. This foundational work laid the groundwork for subsequent innovations. By 2022, Lee and Kumar integrated deep learning techniques with the gradient-based approach, employing deep neural networks to optimize cascaded channels faster [33]. Simultaneously, data rate prediction techniques gained momentum. Founded on the correlation between channel coefficients and achievable data rates, Park et al. (2021) introduced a methodology that presented refined transmission policies tailored for cascaded channels [34]. Expanding on these advancements, Zhao et al. (2023) introduced a fusion of convolutional neural networks with traditional methodologies, resulting in a significant leap in data rate prediction accuracy for cascaded scenarios [35].

1.4. Challenges and Contribution

Effective communication relies heavily on channel estimation, and various techniques have been devised over the years. While deterministic methods were once predominant, they are now deemed insufficient to address the intricacies introduced by RIS-MIMO systems [25]. Sanghvi and Bhat's (2021) research presented an advanced deterministic model for individual channel behaviors but encountered challenges in dynamic scenarios [26].

In the context of individual channel scenarios, the environment was distinctive yet equally dynamic. Martinez and Chen (2021) highlighted the nuanced challenges associated with phase shift optimization, introducing an iterative algorithm to accommodate individual channels' dynamism [36]. Building on this foundation, Ali and Gupta (2022) took further strides by incorporating reinforcement learning into existing methodologies, providing dynamic phase shift adjustments customized for Tx-RIS and RIS-Rx channels [37]. Concurrently, in data rate prediction, Khan and Raza (2022) proposed an RNN-based technique uniquely tailored for individual channels, addressing their inherent temporal dynamics [38]. This sequence of innovations culminated in 2023 when a collaborative effort led by Fernández et al. revealed a robust model that integrated CNNs with RNNs, tailored explicitly for individual channels, marking a significant milestone in data rate prediction methodologies [39].

This research paper considers a wireless communication system assisted by Reconfigurable Intelligent Surfaces (RIS). It introduces a novel RIS architecture and deep learning-based approaches for designing the RIS

reflection matrix with minimal training overhead. To elaborate, the critical contributions of this paper are outlined as follows:

To model channel time frequency response as a 2D image, we used a 5G Link level-based RIS-MIMO MATLAB 2023a simulator.

We present a new approach to channel estimation through deep learning architectures explicitly designed for RIS-MIMO systems. These architectures are uniquely designed to address the challenges posed by having active/passive elements in the RIS. This paper studies a two-stage channel estimation method for the RIS-MIMO communication system. The cascaded MIMO channel between the BS-RIS-UE is estimated in the first stage, whereas the BS-RIS and RIS-UE channels are estimated in the second stage.

This research article proposes two efficient deep neural networks (PS-CNN and BA-CNN) called Net 1 and Net 2, respectively. The first network can solve phase reflection complexity to find optimal phase shifts and optimize the RIS phase shift matrix during the training phase of the reflected signals in RIS elements. This leads to maximizing Signal power/ SNR at the receiver. The second network can achieve a high data rate.

We focus on maximizing the performance of RIS-MIMO systems even when only a handful of RIS elements are active by optimizing the phase of the reflected signal using the RIS controller in active elements.

This paper compares cascaded and individual estimation methods in RIS-MIMO using a set of performance metrics such as accuracy, capacity, path loss, channel gain, and normalized mean square error. The subsequent sections of this document are structured as follows: Section 1 introduces the paper. Section 2 provides background information and discusses related work. Section 3 outlines the system and channel models utilized in this paper, formally defining the primary problem – the design of the LIS interaction matrix. Section 4 introduces and explores the innovative sparse LIS architecture, incorporating a deep learning model for optimal phase shift and high-capacity data rate. Section 5 details the simulation results. Lastly, Section 6 concludes the paper by summarizing the findings and offering concluding remarks.

2. System and channel models

2.1. SYSTEM MODEL

In this work, we have adopted a passive/active RIS architecture with a few RF chains-based MIMO communications systems. Both the transmitter and the receiver are equipped with multiple antennas.

While the terminology utilized in this article operates under the assumption of downlink communication, in which the user terminal (UT) serves as the receiver and the base station (BS) represents the transmitter, two source nodes, S , are equipped with N antennas, two destination nodes D have M antennas, and the RIS has K reflecting active/passive elements. Assuming that severe blocking or deep fading prevents a direct connection between S and D , the channel efficiency between the n th antenna at S and the k th RIS element conforms to Rician fading as follows:

$$H_{T,K} = \sqrt{\frac{K_{k,n}}{K_{k,n}+1} h_{k,n}^{(LOS)}} + \sqrt{\frac{K_{k,n}}{K_{k,n}+1} h_{k,n}^{(NLOS)}}, \quad (1)$$

Where $K_{k,n}$ is the Rician factor for the corresponding link, $h_{k,n}^{(LOS)}$ and $h_{k,n}^{(NLOS)}$ are the line-of-sight (LOS) and non-line-of-sight (NLOS) parts of the fading channel, respectively. for the LOS component, the expression is as follows:

$$h_{k,n}^{(LOS)} = e^{-j(k-1)\pi \sin \theta} d_{k,n}^{-\frac{\alpha}{2}}, \quad (2)$$

where θ is the angle of arrival at the RIS, and β_0 is the path loss at the reference distance of one meter. For the NLOS, we have $h_{k,n}^{(NLOS)} = \tilde{h}_{k,n} d_{k,n}^{-\frac{\alpha}{2}}$ where $\tilde{h}_{k,n}$ models the complex Gaussian small-scale fading with zero mean and unit variance. The channel between the k th RIS element and the m th antenna at D is denoted as $H_{K,R}$ which is similarly modeled. The received signal at the destination is given by

$$y = H_{T,K} \Theta H_{K,R} \chi + \eta, \quad (3)$$

In this context, \mathbf{Y} belongs to the $\mathbb{C}^{M \times 1}$, $H_{K,R} \in \mathbb{C}^{M \times K}$, channel matrix representing the communication link between the Reconfigurable Intelligent Surface (RIS) and the destination node (D), \mathbf{n} belongs to the $\mathbb{C}^{M \times 1}$ space and signifies the additive noise between the source node (S) and the RIS. Additionally, $H_{T,K} \in \mathbb{C}^{N \times K}$, channel vector representing the white Gaussian noise (AWGN) with variance σ^2 , and Θ represents the phase shift matrix at the RIS. The expression for Θ is given by

$$\Theta = \text{diag}(a_1 e^{j\theta_1}, \dots, a_1 e^{j\theta_k}), \quad (4)$$

Here a^k represents the amplitude, and θ^k denotes the phase shift at the k th reflecting element. While a^k is assumed to be constant in numerous existing approaches, it can also vary, as indicated in [29], [30]. In this correspondence, we adopt discrete phase shifts with R-bits quantization, signifying that each Reconfigurable Intelligent Surface (RIS) element has 2^R possible phase shifts.

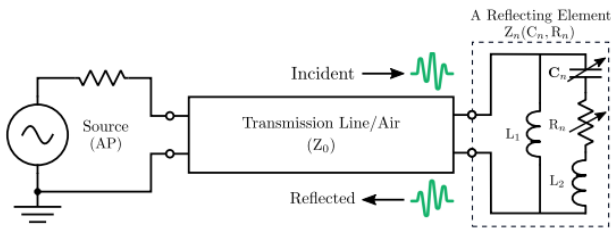


Fig. 1. Transmission line model of a reflecting element.

2.1.1 Cascaded Channel Estimation

We assume the source node (S) receives channel assessments from the destination node (D) through backhaul connections. In certain situations, S directly estimates the channels from $D \rightarrow S$ and deduces the coefficients for the channel from $S \rightarrow D$ through channel reciprocity. The channel estimation method outlined in this section is readily applicable in both scenarios, facilitated by the assumption of

having numerous antennas at both the source and destination nodes. (1)

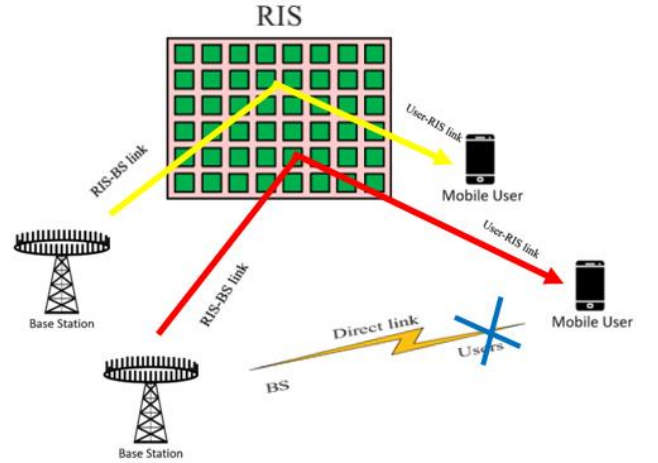


Fig. 2. Show Scenario 1 Direct Cascaded Channel.

(3) By defining the cascaded channel coefficient as $f_{n,k,m} = h_{n,k} h_{k,m}$, like in figure 2 the resulting cascaded channel vector between the n th antenna at the source node (S) and the m th antenna at the destination node (D) is given by:

$$f_{n,m} = [f_{n,1,m}, \dots, f_{n,k,m}]^T, \quad (5)$$

The definition of the cascaded channel vector for the m th receiving antenna at the destination node (D) is as follows:

$$f_m = [f_{1,m}^T, \dots, f_{N,m}^T]^T, \quad (6)$$

Then (3) is expressed as

$$y = F \chi_\varnothing + \eta, \quad (7)$$

where $\mathbf{F} = [\mathbf{f}_1, \dots, \mathbf{f}_M]^T \in \mathbb{C}^{N \times K \times M}$, which is the cascaded channel matrix between S and D, $\chi_\varnothing = \mathbf{x} \otimes \Phi_\varnothing$ is the Kronecker product, $\Phi_\varnothing = [\varnothing_1, \dots, \varnothing_k]^T$ and \varnothing_k is the k th diagonal element of Θ .

Considering equation (7) as a MIMO model with dimensions NK -by- M and assuming the availability of P snapshots of pilots for channel estimation, we obtain:

$$\mathbf{Y} = \mathbf{F} \mathbf{X}_\varnothing + \Gamma, \quad (8)$$

where $\mathbf{Y} = [\mathbf{y}(1), \dots, \mathbf{y}(P)]$, $\mathbf{X}_\varnothing = [\mathbf{X}_\varnothing(1), \dots, \mathbf{X}_\varnothing(P)]$, and $\Gamma = [\boldsymbol{\eta}(1), \dots, \boldsymbol{\eta}(P)]$. The least-square estimation of \mathbf{F} is obtained as

$$F_{LS} = \mathbf{Y} \mathbf{X}_\varnothing^H (\mathbf{X}_\varnothing \mathbf{X}_\varnothing^H)^{-1}, \quad (9)$$

The pilots used for the estimation of the cascaded channel encompass both the transmit signal (x_n) and the phase shift \varnothing_k ; these need to be combined and designed in a way that satisfies $P \geq NM$ and $\mathbf{X}_\varnothing \mathbf{X}_\varnothing^H$ where $P_s/N.I$ represent the power constraint at the source node (S).

2.1.2 Individual Channel Estimation

In this context, we introduce the ICE method, which initially deduces the Channel State Information (CSI) of the base station (BS)-Reconfigurable Intelligent Surface (RIS)

and RIS-user channels separately based on the received training signals. Subsequently, these estimations are employed to reconstruct the cascaded channels. The base station (BS) and user equipment (UE) have M and N antenna arrays. The Reconfigurable Intelligent Surface (RIS) consists of K active/passive elements, or unit cells, capable of individually adjusting their reflection coefficients (i.e., phase shifts). The system model is depicted in Figure 4, and the received signal is expressed as per [31]:

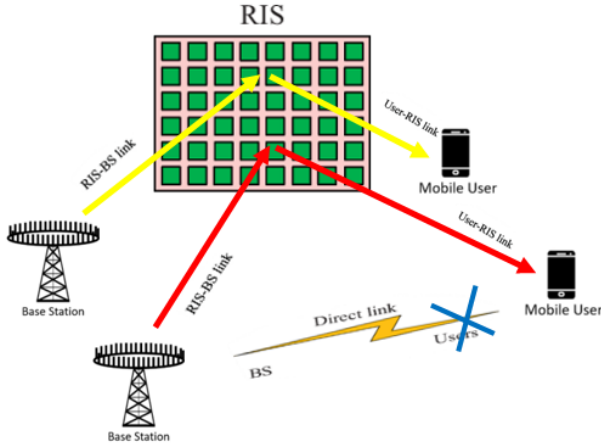


Fig. 3. Show Scenario 2 Separate Cascaded Channel.

$$y[t] = H_{T,K} (s[t] \square H_{K,R} x[t] + \eta[t]), \quad (10)$$

Where $x[t] \in \mathbb{C}^{M \times 1}$ is the vector containing the transmitted pilot signals at time t , as shown in figure 3, $s[t] = [s_{1,e^{j\theta_1}}, \dots, s_{N,e^{j\theta_N}}]^T \in \mathbb{C}^{N \times 1}$ is the vector that models the phase shifts, and activation controls the on-off state of the corresponding element at time t . The matrices $H_{T,K} \in \mathbb{C}^{N \times K}$ and $H_{K,R} \in \mathbb{C}^{K \times M}$ denotes the BS-RIS and RIS-UE MIMO channels, respectively. In contrast, $\eta[t] \in \mathbb{C}^{N \times 1}$ is the additive white Gaussian noise (AWGN) vector.

$$Y = H_{T,K} (S \square (H_{K,R} X)) + \eta, \quad (11)$$

2.2. Channel model

In this paper, we employ a wideband geometric channel model for the channels $H_{T,K}$, and $H_{K,R}$ between the transmitter/receiver and the Reconfigurable Intelligent Surface (RIS). The channel estimation process in RIS-MIMO systems poses more significant challenges than conventional active device-based MIMO systems. This is attributed to the following factors. Firstly, CSI can be acquired by transmitting training sequences in an active device-based system. However, in the case of RIS-assisted systems, channel estimation is limited to active transceivers only, as the RIS itself is a passive device without active transmitting and receiving capabilities.

Moreover, Reconfigurable Intelligent Surfaces (RIS) frequently incorporate many Reconfigurable Elements (REs), leading to a significant training overhead. In summary, independently recovering the Channel State Information (CSI) for the transmitter-RIS and RIS-receiver channels is challenging due to their interdependence with the reflection coefficient matrix. To address these challenges, researchers are exploring innovative approaches to estimate the cascaded

channel, encompassing both the RIS-receiver and transmitter-RIS channels.

We will analyze a typical case to clarify the reasoning behind estimating cascaded channels for optimizing combined active and passive beamforming in RIS-MIMO systems. This investigation explores a multi-user Multiple Input Multiple Output (MIMO) system, where a Reconfigurable Intelligent Surface (RIS) aids a base station (BS) equipped with multiple antennas, providing support to numerous users with various antennas each. The channels $H_{T,K}$, and $H_{K,R}$, represent the responses from the BS to the RIS and the RIS to the k th user, respectively. Additionally, $H_{T,K}$, represents the channel response from the BS to the k th user. The entire channel response from the BS to user k is expressed as $H_{T,K} \text{diag}(v) H_{K,R} = v^T \text{diag}(H_{K,R}) H_{T,K}$, where $\text{diag}(v)$ is the reflection coefficient matrix. Consequently, the only prerequisite for the joint design of active beamforming at the BS and the passive reflection coefficient matrix $\text{diag}(v)$ at the RIS is the cascaded channel's Channel State Information (CSI).

$$H_K = \text{diag}(H_{K,R}) H_{T,K}, \quad (12)$$

As a result, this research will not tackle the Channel State Information (CSI) of the direct link, as it can be handled using conventional estimation techniques within the Multiple Input Multiple Output (MIMO) system. Thus, the main challenge in channel estimation stems from the cascaded channel estimation approach, recognized as the primary focus in recent scholarly works. Broadly, the latest methods for cascaded channel estimation can be categorized into two groups: direct cascaded channel estimation (DCCE) or separate cascaded channel estimation, depending on whether they perform a direct or indirect estimate of the cascaded channel (SCCE).

We aim to formulate the Reconfigurable Intelligent Surface (RIS) interaction vector, denoted as $\psi \in \mathbb{C}^{M \times 1}$ (reflecting beamforming vector), to maximize the achievable rate at the receiver. This can be expressed as:

$$R = \frac{1}{k} \sum_{k=1}^k \log_2 (1 + \text{SNR} | H_{T,K}^T \Psi H_{K,R}^T |^2) \quad (13)$$

where $\text{SNR} = PT / (k \sigma_n^2)$ represents the signal-to-noise ratio. As mentioned in Section III, every element in the RIS reflection beamforming vector, Ψ , is implemented using an RF phase shifter. These phase shifters, however, usually have a quantized set of angles and cannot shift the signal with any phase. To capture this constraint, we assume that the reflection beamforming vector Ψ can only be picked from a predefined codebook ρ . Every candidate reflection beamforming codeword in ρ is supposed to be implemented using quantized phase shifters.

In Fig. 4. the proposed RIS architecture is exposed, where K active/passive channel sensors are randomly distributed over the RIS. These active elements have two modes of operation: (i) a channel sensing mode, which is connected to the baseband and is used to estimate the channels, and (ii) a reflection mode, where it just reflects the

incident signal by applying a phase shift. The rest of the RIS elements are passive reflectors not connected to the baseband.

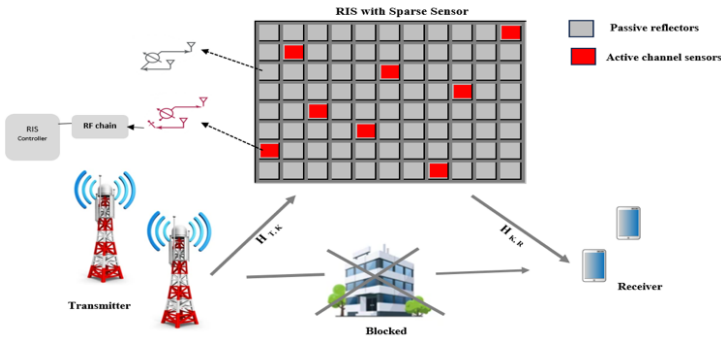


Fig. 4. The proposed RIS architecture

2.3. Channel estimation, Phase Shift, and Beamforming Based on Direct Cascaded Channel

In RIS-MIMO communication systems, especially when considering cascaded channels, both phase shifts at the RIS and beamforming at the transmitter and receiver play pivotal roles.

2.3.1 Channel estimation:

Passive RIS: The transmitter sends a known pilot signal $x(t)$ through the cascaded channel ($H_{t,k} \times H_{k,r}$) to the RIS. In RIS, the signal will be reflected toward the receiver. The reflected signal $y(t)$ at the receiver is a combination of the transmitted pilot signal $x(t)$, the effect of the cascaded channel ($H_{t,k} \times H_{k,r}$), and noise $n(t)$ will be $y(t) = (H_{t,k} \times H_{k,r}) \cdot x(t) + n(t)$. The receiver estimates the cascaded channel ($H_{t,k} \times H_{k,r}$) by comparing the known transmitted signal $x(t)$ with the received signal $y(t)$ by using standard channel estimation techniques, such as least squares, then the estimation of the channel will be at the receiver as shown in figure 5.



Fig. 5. Show Direct Cascaded Channel estimation one time at the receiver.

- **Active RIS:** In active channel estimation, the RIS elements are configured to emit known signals. The transmitter and the RIS work together. The transmitter sends available pilot signals towards the RIS, and the RIS actively modifies these signals using its elements before they are reflected towards the receiver. The receiver captures the signals modified by the RIS and uses them for channel estimation. In active channel estimation, the channel estimation process typically considers the combined effect of the channels from the transmitter to the RIS ($H_{t,k}$) and from the RIS to the receiver ($H_{k,r}$), including the influence of the

RIS's active elements. The RIS elements actively participate in the estimation process by modifying the transmitted signals.

2.3.2 Phase Shift at the RIS:

The primary role of the RIS in the communication process is to introduce controllable phase shifts to the incident signals to enhance the communication link's quality. When the cascaded channel approach is employed:

The total channel $H_{T,K,R}$ combines the transmitter-to-RIS channel, the RIS's phase shifts, and the RIS-to-receiver channel.

Passive RIS elements cannot actively manipulate or control the phase of the incident signal in real time. Their primary function is to reflect and adjust the phase of the incoming signal based on their predefined characteristics. The phase shift introduced by passive RIS is a static property and does not change during signal transmission.

Active RIS elements, on the other hand, can actively and dynamically control the phase of the incident signal in real-time. In contrast, the reflection phase can be controlled by switching the on-off state of the PIN Diode in RIS sensors. They can adaptively adjust the phase to optimize signal quality, reduce interference, and steer the signal to specific directions based on real-time conditions.

The optimal phase shift matrix Φ is derived to maximize the signal-to-noise ratio (SNR) or any other defined performance metric at the receiver. The optimization problem can be formulated as:

$$\max_{\Phi} |H_{K,R} \Phi H_{T,K}|^2 \quad (14)$$

Subject to constraints on the phase shifts θ_i , typically within $[0, 2\pi]$.

2.3.3 Beamforming:

Beamforming in wireless communication refers to directing the transmission or reception of signals in specific directions. Instead of sending signals uniformly in all orders, beamforming uses multiple antennas to shape the radio waves in a particular direction, enhancing signal quality and mitigating interference from other sources. Beamforming strategies can be employed at both the transmitter and the receiver to shape the transmitted and received signals further:

Transmitter Beamforming (Precoding): Given the cascaded channel's knowledge, the transmitter can shape the signals to add up constructively at the intended receiver while minimizing interference to other potential receivers.

Receiver Beamforming (Decoding): At the receiver's end, beamforming can amplify the intended signal while minimizing interference and noise.

In a system with passive RIS elements, the primary responsibility for beamforming lies with the transmitter. The transmitter adjusts the phase of the incident signal to focus it in the desired direction. The passive RIS elements reflect and adjust the phase based on their predetermined characteristics.

In a system with active RIS elements, both the transmitter and the active RIS elements are involved in beamforming. The transmitter initiates the beamforming process by adjusting the phase of the incident signal, and the active RIS elements further fine-tune and actively control the signal phase to optimize its direction.

The optimal beamforming vectors (for both transmission and reception) can be derived by solving optimization problems that maximize the received signal power or the SNR, considering the cascaded channel's effects.

2.3.4 Joint Optimization:

In practice, optimal performance can often be achieved by jointly optimizing both the RIS phase shifts and the beamforming vectors. This joint optimization would involve the following:

$$\max_{\varnothing, w, v} |v^H H_{K,R} \varnothing H_{T,K} w|^2 \quad (15)$$

Where w is the transmitter beamforming vector, and v is the receiver beamforming vector. This formulation seeks to maximize the combined system gain from the RIS phase shifts and MIMO beamforming.

2.4. Channel Estimation, Phase Shift, and Beamforming Based on Separate Cascaded Channel

2.4.1 Channel Estimation:

Passive RIS: First, Estimating the transmitter-to-RIS channel $H_{T,K}$, the transmitter sends a known pilot signal $x(t)$ through the channel $H_{T,K}$ to the passive RIS. This signal remains unaltered by the RIS. The RIS receives the transmitted pilot signal. The received signal $y_h(t)$ at the RIS can be modeled as $y(t) = H_{T,K} \cdot x(t) + n(t)$, Where $n(t)$ represents the noise at the RIS. We used standard channel estimation techniques, such as the least squares estimator, to estimate $H_{T,K}$. Second, Estimating the RIS-to-Receiver Channel $H_{K,R}$, the transmitter sends a known signal $x(t)$ toward the passive RIS. The signal $y(t)$ received at the receiver is a combination of the transmitted signal $x(t)$, the effect of $H_{K,R}$, and noise $n(t)$: $y(t) = H_{K,R} \cdot x(t) + n(t)$. we estimated the $H_{K,R}$ using standard channel estimation techniques, similar to the estimated $H_{T,K}$, and then the estimation of the channel will be at the RIS device sensing and the receiver as shown in Figure 6.

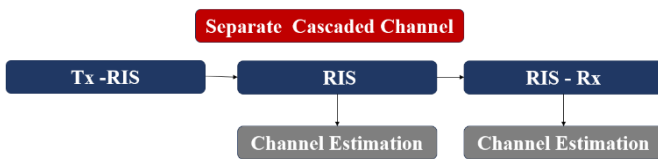


Fig. 6. Show Separate Cascaded Channel estimation twice at the RIS and the receiver.

Active RIS: The estimation process for active RIS elements is quite similar to that of passive RIS. The main difference is that the RIS elements actively modify the signals in active RIS. The estimation steps for h and g in an active RIS are the same as for passive RIS, as both rely on measuring the effect of the channels $H_{T,K}$, and $H_{K,R}$ with the active contribution of the RIS in modifying signals.

The goal in both passive and active RIS scenarios is to estimate the separate channels $H_{T,K}$, $H_{K,R}$, and H_R to understand the effects of the RIS on the transmitted and received signals and to calculate the corresponding channel coefficients.

2.4.2 Phase Shift at the RIS:

In a separate or individual channels approach, the RIS optimizes its phase shifts based on the transmitter-to-RIS channel and the RIS-to-receiver channel.

For the transmitter-to-RIS channel $H_{T,K}$, the RIS aims to capture the signal from the transmitter most effectively. It might optimize the phase shifts such that the received signal strength at the RIS is maximized.

Passive RIS elements introduce a static phase shift to the incident signals in separated channels. This phase shift is determined by the physical configuration and design of the passive elements and remains constant during signal transmission. Passive RIS elements in separated channels cannot dynamically adapt the phase of the incident signals in real-time. They cannot respond to changing channel conditions, user positions, or dynamic optimization criteria for phase control.

Active RIS elements can actively and dynamically control the phase of the incident signals in real time in separated channels. This dynamic control allows for instantaneous changes in phase to optimize signal transmission. It can also adapt the phase of the signals based on changing conditions, allowing for dynamic phase adjustments that respond to real-time variations in the environment, user positions, or communication requirements.

For the RIS-to-Receiver channel $H_{K,R}$, the RIS focuses on optimally reflecting the incident signals towards the receiver. The phase shifts can be configured to ensure the signals are constructively combined at the receiver.

$$\max_{\varnothing} |H_{T,K} \varnothing|^2 \quad (16)$$

And

$$\max_{\varnothing} |H_{K,R} \varnothing|^2 \quad (17)$$

subject to the typical constraints on the phase shifts \varnothing within $[0, 2\pi]$

2.4.3 Beamforming:

Transmitter Beamforming (Precoding): With knowledge of the transmitter-to-RIS channel, the transmitter can employ beamforming to maximize the signal strength at the RIS.

Receiver Beamforming (Decoding): Conversely, given the RIS-to-receiver channel, beamforming at the receiver can ensure that the reflected signals from the RIS are constructively combined, enhancing the desired signal quality.

For passive RIS, the transmitter is primarily responsible for beamforming, whereas for active RIS, both the transmitter and the active RIS elements contribute to the beamforming process. The choice between passive and active RIS depends on the specific requirements of the communication system and the level of control and adaptability needed for beamforming.

The optimal beamforming vectors can be derived for each channel to maximize the received signal power or the signal-to-noise ratio (SNR).

2.4.4 Joint Optimization:

Optimally, to exploit the full potential of the RIS-MIMO system with individual channels, a joint optimization of both RIS phase shifts and beamforming vectors for each

channel is required. The joint optimization can be formulated as follows:

$$\max_{\Phi, w, v} (v^H H_{K,R} \Phi w) (w^H H_{T,K} \Phi v) \quad (18)$$

Here, w denotes the transmitter beamforming vector, and v signifies the receiver beamforming vector. This optimization maximizes the system gain from each channel's RIS phase shifts and MIMO beamforming.

3. Deep learning model design for optimal phase shift and high-capacity data rate

3.1 Deep Learning Structure

As seen in Figure 7, the new learning model comprises two deep neural networks, Net1 and Net2. Net1 serves as the primary network. The system inputs are $N \times M \times K$ and represent each entry in a cascaded K group of $2R$ dimensional category vectors. Each group represents the discrete phase shift of R bits at a single RIS element.

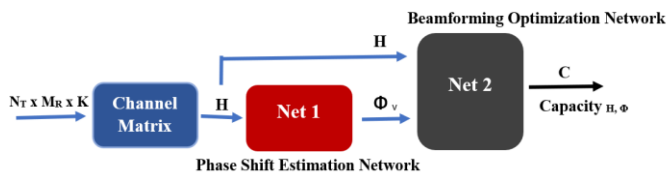


Fig. 7. The deep learning network structure.

Training Net1 using standard supervised learning is challenging because of the unavailability of labeled data, namely the optimal phase shifts. Conversely, employing the brute-force search method to identify the optimal phase shifts for a reasonably large RIS element number K and phase quantization bit number R may prove computationally unfeasible. There would be 2^{KR} potential phase shifts for each channel realization. To solve this problem, the complement neural network Net2 is introduced. The inputs to Net2 are F and Φ_v ; the output is the corresponding capacity $C_{F, \Phi}$.

3.1.1 First Deep Learning Model - Phase Shift Estimation Network:

The primary objective of the Phase Shift Estimation Network is to predict the optimal phase shift values leveraging the channel matrix and RIS elements. The neural network commences with an input layer comprising many nodes equivalent to the sum of the channel coefficients from the channel matrix and the RIS elements without any activation function. Progressing deeper, the network hosts three hidden layers. The first hidden layer has 128 nodes and employs the ReLU activation function. The subsequent layer amplifies its complexity with 256 nodes using the ReLU activation. The third and final hidden layer reverts to 128 nodes, maintaining the ReLU activation. The culmination of this network is the output layer. It houses many nodes equal to the RIS elements, each indicating an optimal phase shift value for a particular element. Considering the nature of phase shifts, the Tanh activation function is an appropriate choice, especially if phase shift values are bound between $-\pi$ and π . Alternatively, a Sigmoid activation function is preferable if the phase shifts are normalized between 0 and 1. The Mean Squared Error (MSE) loss function measures the model's accuracy.

Input Layer:

Size: Number of channel coefficients (from the channel matrix) + Number of RIS elements $N \times M \times K$.

Type: Dense (fully connected).

Hidden Layers:

Multiple hidden layers using activation functions ReLU. The depth and width of these layers can be adjusted based on the complexity of the channel.

Output Layer:

Size: Number of RIS elements (representing each element's optimal phase shift values).

Type: Dense with a linear or sigmoid activation, depending on the phase range.

Loss Function: Mean Squared Error (MSE) for regression of the optimal phase shifts.

3.1.2 Second Deep Learning Model - Beamforming Optimization Network:

Entering into a field of data rate predictions, the Beamforming Optimization Network aims to predict the high-capacity data rate, building upon the optimal phase shifts derived from the previous model and the channel matrix. The initiation of this network is marked by an input layer that integrates nodes equivalent to the sum of the channel coefficients from the channel matrix and the optimal phase shift values without any activation function. The network encompasses four hidden layers to effectively capture the complexities of predicting data rates. The first layer has been designed with 256 nodes, accompanied by the ReLU activation function. This is followed by a more intricate layer boasting 512 nodes, yet continuing with the ReLU activation. The network then scales down with the third layer, presenting 256 nodes and persisting with the ReLU activation. The fourth and concluding hidden layer scales to 128 nodes, retaining the ReLU activation. The pinnacle of this network is an output layer with a singular node, symbolizing the high-capacity data rate value, and aptly, it uses a linear activation function. Given the regression nature of this prediction, the Mean Squared Error (MSE) loss function stands as the chosen metric to evaluate the model's performance.

Input Layer:

Size: Number of channel coefficients (from the channel matrix) + Number of optimal phase shift values HF, Φ_v .

Type: Dense.

Hidden Layers:

Similar to the first model but tailored to handle the increased complexity of predicting data rates.

Output Layer:

Size: 1 (representing the predicted data rate).

Type: Dense with a linear activation (since the data rate is continuous).

Loss Function: MSE or any suitable regression loss, depending on the nature of the data.

3.2 Train the Deep Neural Networks

3.2.1 Train Cascaded Channel:

Algorithm 1: Phase Shift Estimation for Cascaded Channel

Procedure Train Phase Shift Cascaded

1. **Input:** dataset consisting of $H_{T,K,R}$ (Cascaded Channel matrix), K (RIS elements), Φ_{true} (True phase shifts)
2. $i = 0$ (initial epoch)
3. **Output:** Φ (Estimated optimal phase shifts)
4. **Begin:**
5. Initialize Cascaded Network: Input ($|H_{T,K,R}| + |K|$ nodes) \rightarrow Hidden Layers \rightarrow Output ($|K|$ nodes)
6. Initialize optimizer (e.g., Adam)
7. Initialize loss function = Mean Square Error
8. While $i < \text{max epochs}$:
9. For each batch in a dataset:
10. Extract batch $H_{T,K,R}$, batch K , batch Φ_{true} from batch
11. $\Phi =$ Cascaded Network forward (batch $H_{T,K,R}$, batch K)
12. $\text{loss} = \text{loss function}(\Phi, \text{batch } \Phi_{\text{true}})$
13. Backpropagate loss and update network weights using an optimizer
14. End For
15. $i = i + 1$
16. End While
17. **Return** Φ
18. End Procedure

Algorithm2: Beamforming Optimization for Cascaded Channel

Procedure Train Beamforming Cascaded

1. **Input:** dataset consisting of $H_{T,K,R}$ (Cascaded Channel matrix), Φ_{cascaded} (Phase shifts for a cascaded channel from the previous network), C_{true} (True data rates)
2. $i = 0$ (initial epoch)
3. **Output:** C (Estimated high capacity (data rates))
4. **Begin:**
5. Initialize Beamforming Network Cascaded: Input ($|H_{T,K,R}| + |\Phi_{\text{cascaded}}|$ nodes) \rightarrow Hidden Layers \rightarrow Output (1 node for data rate)
6. Initialize optimizer (e.g., Adam)
7. Initialize loss function = Mean Square Error
8. While $i < \text{max epochs}$:
9. For each batch in a dataset:
10. Extract batch C_{cascaded} , batch Φ_{cascaded} , batch C_{true} from batch
11. $C =$ Beamforming Network Cascaded forward (batch C_{cascaded} , batch Φ_{cascaded})
12. $\text{loss} = \text{loss function}(C, \text{batch } C_{\text{true}})$
13. Backpropagate loss and update network weights using an optimizer
14. End For
15. $i = i + 1$
16. End While
17. **Return** C
18. End Procedure

3.2.2 Train Separate Channel:

Algorithm 3: Phase Shift Estimation for Separate Channel

Procedure Train Phase Shift Separate

1. **Input:** dataset consisting of $H_{T,K}$ (Transmitter to RIS channel), $H_{K,R}$ (RIS to Receiver channel), R (RIS elements), $\Phi_{\text{true}_{Tx}}$ (True phase shifts for Tx -RIS), $\Phi_{\text{true}_{Rx}}$ (True phase shifts for RIS-Rx)
2. $i = 0$ (initial epoch)
3. **Output:** Φ_{Tx} , Φ_{Rx} (Estimated phase shifts for both channels)
4. **Begin:**
5. Initialize Separate Network Tx : Input ($|H_{T,K}| + |K|$ nodes) \rightarrow Hidden Layers \rightarrow Output ($|R|$ nodes)
6. Initialize Separate Network Rx : Input ($|H_{K,R}| + |K|$ nodes) \rightarrow Hidden Layers \rightarrow Output ($|K|$ nodes)
7. Initialize optimizer (e.g., Adam)
8. Initialize loss function = Mean Squared Error
9. While $i < \text{max epochs}$:
10. For each batch in a dataset:
11. Extract batch $H_{T,K}$, batch $H_{K,R}$, batch K , batch $\Phi_{\text{true}_{Tx}}$, batch $\Phi_{\text{true}_{Rx}}$ from batch
12. $\Phi_{Tx} =$ Separate Network Tx forward (batch $H_{T,K}$, batch K)
13. $\Phi_{Rx} =$ Separate Network Rx forward (batch $H_{K,R}$, batch K)
14. $\text{loss}_{Tx} = \text{loss function}(\Phi_{Tx}, \text{batch } \Phi_{\text{true}_{Tx}})$
15. $\text{loss}_{Rx} = \text{loss function}(\Phi_{Rx}, \text{batch } \Phi_{\text{true}_{Rx}})$
16. Backpropagate loss Tx and update Separate Network Tx weights using an optimizer
17. Backpropagate loss Rx and update Separate Network Rx weights using an optimizer
18. End For
19. $i = i + 1$
20. End While
21. **Return** Φ_{Tx} , Φ_{Rx}
22. End Procedure

Algorithm 4: Beamforming Optimization for Separate Channel

Procedure Train Data Rate Separate

- 1) **Input:** dataset consisting of $H_{T,K}$, $H_{K,R}$, Φ_{Tx} (Phase shifts for Tx -RIS), Φ_{Rx} (Phase shifts for RIS-Rx), C_{true} (True data rates)
- 2) $i = 0$ (initial epoch)
- 3) **Output:** C (Estimated data rates)
- 4) **Begin:**
- 5) Initialize Input Size = $|H_{T,K}| + |H_{K,R}| + |\Phi_{Tx}| + |\Phi_{Rx}|$
- 6) Initialize Data Rate Network Separate: Input (Input Size nodes) \rightarrow Hidden Layers \rightarrow Output (1 node for data rate)
- 7) Initialize optimizer (e.g., Adam)
- 8) Initialize loss function = Mean Squared Error
- 9) While $i < \text{max epochs}$:
- 10) For each batch in a dataset:
- 11) Extract batch $H_{T,K}$, batch $H_{K,R}$, batch Φ_{Tx} , batch Φ_{Rx} , batch C_{true} from batch
- 12) combined input = concatenate (batch $H_{T,K}$, batch $H_{K,R}$, batch Φ_{Tx} , batch Φ_{Rx})
- 13) $C =$ Data Rate Network Separate forward (combined input)
- 14) $\text{loss} = \text{loss function}(C, \text{batch } C_{\text{true}})$
- 15) Backpropagate loss and update network weights using an optimizer
- 16) End For

- 17) $i = i + 1$
- 18) End While
- 19) **Return C**
- 20) End Procedure

4. SIMULATION RESULTS

This section assesses the effectiveness of the two time-scale learning techniques presented. The simulation results are shown following a description of the channel environment configuration. We examine a RIS-assisted network in which $M = 2$ two-antenna users are connected to two BSs equipped with $N = 2$ antennas via a RIS with $K_{\text{active}}=8$ and $K_{\text{passive}}=80$ components, table 1 shows all the simulation parameters used in two scenarios.

Table 1 The parameter setup for the RIS scenario.

Parameters	Values
MIMO, RIS, BS, UE	2 x 2, 1,2,2
Distance of RIS-BS	100m
Simulation	Downlink
RIS Controller BS	BS1,BS2
The Nearest Distance between users and BS	102m
Links	BS1:RIS1*60,RIS1:UE1*110 BS2:RIS2*60,RIS2:UE2*110
Reflect Coefficient RIS	1
User Velocity	50 m/s
Width of Reflecting Elements	0.012m
Length of Reflecting Elements	0.012m
No.Elements RIS	{8,16}
Type of modulation	OFDM 64 QAM
Maximum Doppler frequency	36 Hz, 200 Hz
Noise model	Gaussian Noise
Sample frequency	3.84 MHz
No. of Sub-carriers	72
Time Slot	14
Fading	Rician
Channel Power Delay Profile	TDL-A_45ns
Channel Estimation Method	Pilot Aided LS
Pilot Pattern Downlink	Diamond
Receiver Type MIMO	MMSE
Frame Structure	FDD

To estimate all elements in the cascaded BS-RIS-UE channels, $(N + 1) \times K$ symbol times are required. Assuming users are randomly distributed within a 10 m radius circle, direct links between BS and UE are blocked (as depicted in Fig. 2). In all simulations described below, the channels exhibit Rician fading with a Rician factor $K_{k,n}$ of 10 dB. Additionally, the phase shifts at every RIS element are quantized using three bits. Figure 8 illustrates the capacities of the RIS-MIMO network, featuring two antennas at the source and two at the destination. The results are shown for RIS elements with different quantities of K , namely 8, 32, and 64. The results shown in Figure 8 demonstrate that both cascade and individual channels achieve high data rates about

the signal-to-noise ratio, which is an impressive performance. As the quantity of elements (K) present in the reflecting surface increases, so does the capacity. They approached the ideal scenario where $K = 8$ and the cascade channel estimate performed better than attempting to anticipate the single channel. By the techniques outlined in Section III, 20,000 frames of training data are produced to train neural networks Net1 and Net2. The average capacities are determined using a set of one thousand independent channel realizations after training. The outcomes of the suggested cascaded and separate approaches at the RIS are shown in Figure 8 for comparison. In every instance, it is evident that the proposed model attains more capabilities than the DDL [45]. We provide the outcome of a brute-force search for the best phase shift, specifically for $K = 8$. It is shown that the performance of the suggested DDL is comparable to that obtained using brute-force search. It is worth noting that getting the brute-force search results for $K = 32$ and 64 is very challenging, if not unattainable, due to the substantial number of potential phase shifts ($23 \times 32 = 296$ or $23 \times 64 = 2192$) that each set of channel realizations would have to traverse.

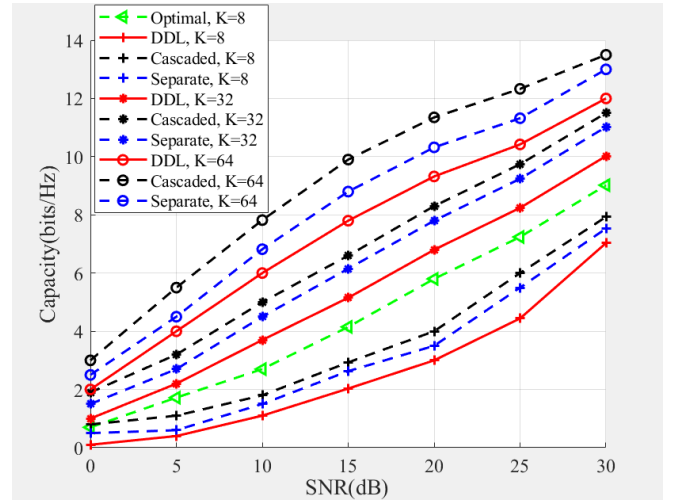


Fig. 8. The capacity in the RIS-MIMO network with two antennas at the source node and two antennae at the destination node for cascaded, separate, double deep learning and optimal channel with different numbers of K elements.

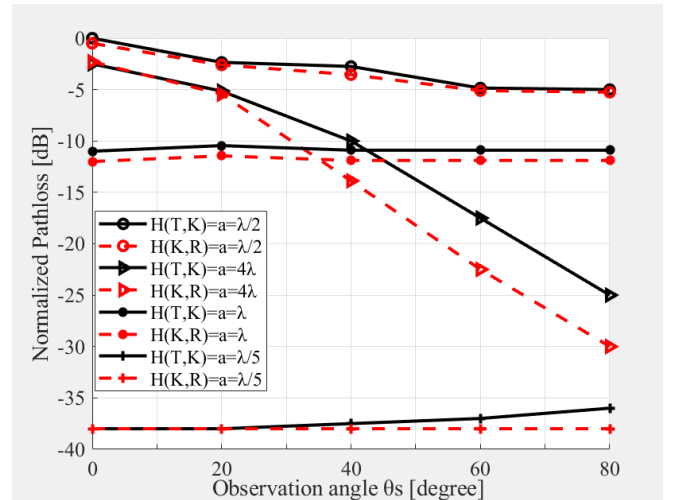


Fig. 9. Shows normalized path loss for two separate channels when the area between the node and another

node(Meta-atom a) is equal to $4\lambda, \lambda, \lambda/2$, and $\lambda/5$ incoming wavelength with different degrees of angle θ_s .

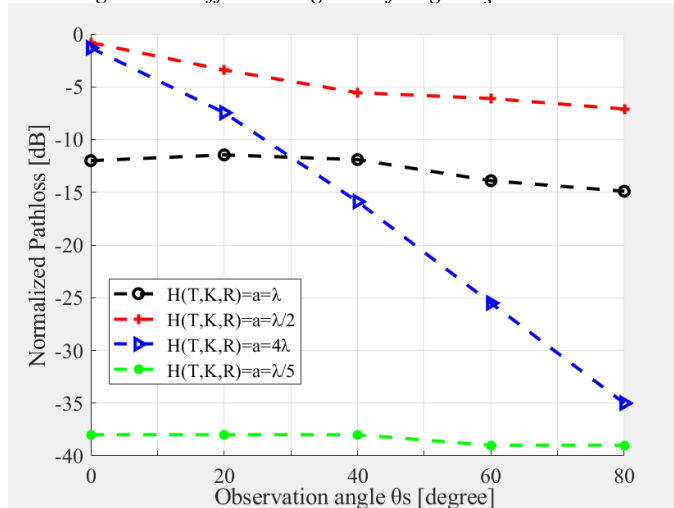


Fig. 10. Shows normalized path loss for cascaded channels when the area between the node and another node (Meta-atom a) is equal to $4\lambda, \lambda, \lambda/2$, and $\lambda/5$ incoming wavelengths with different degrees of angle θ_s .

A similar trend can be seen in Figure 9 and Figure 10, which demonstrates the normalized path loss performance against various observation angle values when $K=8$. The rest of the simulation parameters are the same as in Fig. 8. Note that the spatial correlation in H with $a = \lambda/2$ is higher than when $a = 4\lambda$. Fig. 3 indicates that the path loss performance improves when the channel matrix is spatially less correlated, i.e., for $a = 4\lambda$ case. In both cases, our scheme is preferable as it yields the estimated channels with higher quality. As for when the distance a was equal to the λ wavelength, the path loss was very high, but it was less than the case of $\lambda/2$ wavelength and the worst performance compared to 4λ the wavelength.

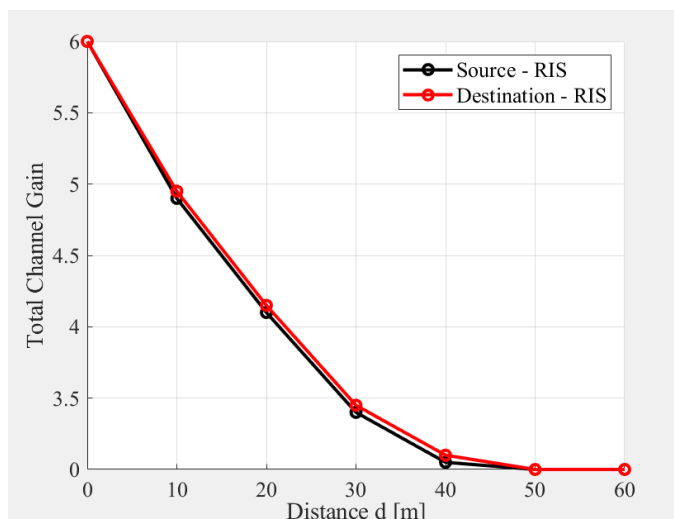


Fig. 11. Shows the total channel gain depending on the distance of the source and destination from the RIS.

We see in Figure 11 that total channel gain is very high when we place the Reconfigurable intelligent surfaces at a distance close to the source or from the destination. The whole channel gain is highest when the reflective surface is entirely close to the source or from the target. That is when the distance between the RIS source and the RIS destination

equals zero. The total channel gain decreases when the distance increases between the reflective surface and the source or the reflective surface and the target.

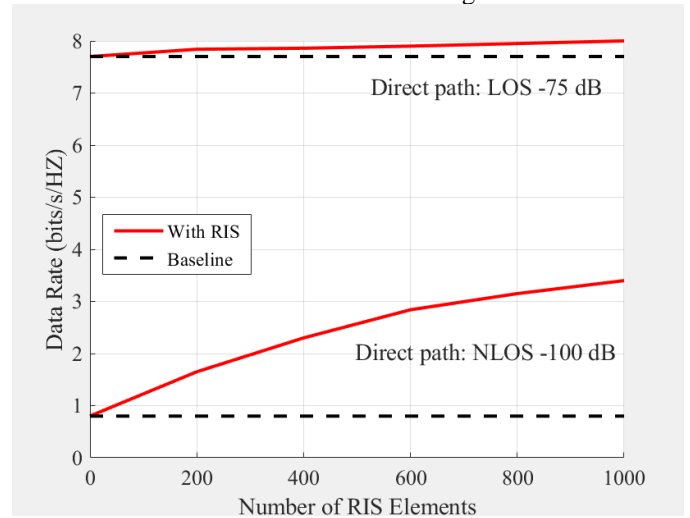


Fig. 12. Illustrate the path LOS and NLOS with RIS and direct path.

Figure 12 Through simulation, we were able to calculate the signal focusing to know the difference between using LOS and NLOS and calculating the amount of data rate. In the first case, when using LOS, if we assume that there is no barrier between the transmitter and the receiver, the data rate will be very high, and even in the case of using reflective surfaces, the data rate will also be very high. The difference between them is small in this case. As for the second case, when using NLOS, if we assume that there is a block between the sender and the receiver, meaning that there is no direct path between them, we will be forced to use the reflective surface route. Here, the real difference will become apparent when using reflective surfaces, as the results give us a higher data rate using the smart reflected surfaces than the regular surface.

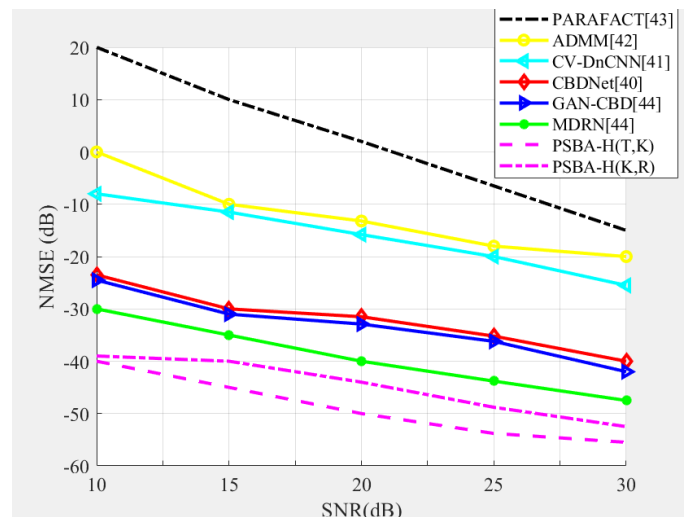


Fig. 13. Illustrate the NMSE performance comparison of ADMM, CV-DnCNN, CBDNet, GAN-CBD, and MRDN with separate CS methods.

Figure 13 compares the NMSE performance of the proposed PSBA-based separate channel estimators for different structures (e.g., CBDNet [40], GAN-CBDN[44], CV-

DnCNN [41], MDRN[44]) and with existing conventional channel estimation methods (e.g., ADMM [42], PAPRFAC [43]). The simulation results average over 400 iterations for the proposed method. It can be observed that PSBA- $H_{T,K,R}$, and PSBA- $H_{T,K}$ can achieve better NMSE performance compared with GAN-CBD and CBDNet by 5.63 dB and 4.51 dB, respectively. Compared with CV-DnCNN, which is also based on CNN, as well as conventional ADMM and PAPRFAC, regardless of the significant performance comparison in NMSE, the lower complexity of PSBA allows it to be better applied.

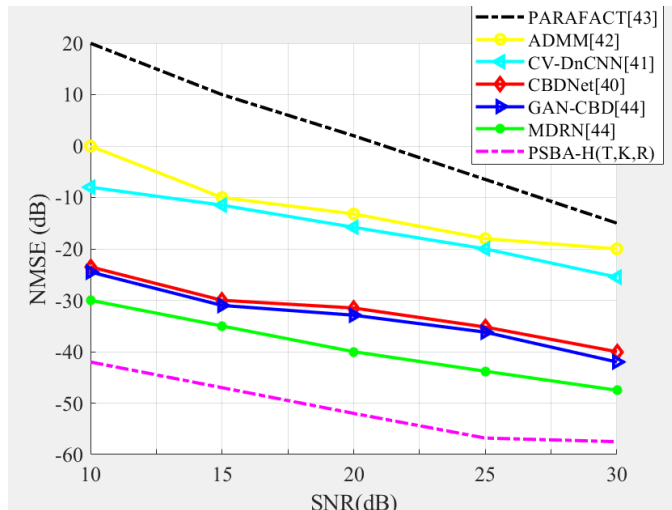


Fig. 14. Illustrate the NMSE performance comparison of ADMM, CV-DnCNN, CBDNet, GAN-CBD, and MRDN with cascaded CS methods.

Figure 14 compares the different models, including the MRDN, CBDNet, and GAN-CBD. We can find that the PSBA- $H_{T,K,R}$ can achieve the best NMSE performance and fastest convergence. Because the PSBA- $H_{T,K,R}$ brings the advantage of judging the network, it performs better than the PSBA- $H_{T,K}$, and PSBA- $H_{K,R}$. The computational complexity of training and offline operation can be hugely reduced. Also, the robustness of the channel estimator to different scenarios is enhanced. The average running time of PSBA- $H_{T,K,R}$ (in seconds) is 0.0073, while the PSBA- $H_{T,K}$ and the PSBA- $H_{K,R}$ are 0.0096 and 0.0092 respectively, the computational complexity of training and offline operations for the PSBA- $H_{T,K,R}$ can be reduced compared with the PSBA- $H_{T,K}$ and the PSBA- $H_{K,R}$. However, for almost the same computational complexity, the PSBA- $H_{K,R}$ can achieve better NMSE performance and fast convergence than the PSBA- $H_{T,K}$. But compared with the PSBA- $H_{T,K,R}$, the improvement of network structure is not significant.

5. CONCLUSION

This letter proposed a new deep-learning network for joint phase shift and beamforming based on cascaded and separate channels in the RIS-MIMO network. We have proposed a two-stage channel estimation scenario for the RIS - MIMO communication system, where the cascaded channel between the BS-RIS-UE is estimated in the first stage, and the separate channel BS-RIS and RIS-UE is estimated in the second stage. We also presented a phase shift design and beamforming for the RIS, which approximately maximizes the channel gain for

the user. We show the effectiveness of the proposed channel estimation methods and phase shift design through numerical simulations. The suggested method demonstrates commendable performance without requiring intricate optimization or resembling reinforcement learning. This quality renders it an appealing approach in the context of RIS phase shift networks and other systems encountering analogous scenarios.

Author Contributions

Walaah Hussein: Conceptualization; methodology; formal analysis; writing—original draft; writing—review and editing. Kamil Audah: Software; validation. Walaah Hussein: Data curation; writing—review & editing.

Acknowledgements

The author is very thankful to the supervisor, prof. Dr. Nor Kamariah Noordin and to the University Putra Malaysia, especially for the Department of Computer and Communications System Engineering, and to the Wireless and Photonic Networks Research Centre of Excellence (WiPNET), Faculty of Engineering and Technology. Conflict of Interest The authors declare no conflict of interest.

Data Availability

The data that support the findings of this study are available from the corresponding author upon reasonable request.

REFERENCES

- [1] M. Jian et al., "Reconfigurable intelligent surfaces for wireless communications: Overview of hardware designs, channel models, and estimation techniques" *Intell. Conver. Netw.*, vol. 3, no. 1, pp. 1–32, 2022.
- [2] S. Fang, G. Chen, and Y. Li, "Joint optimization for secure intelligent reflecting surface assisted UAV networks," *IEEE Wireless Commun. Lett.*, vol. 10, no. 2, pp. 276–280, Feb. 2021.
- [3] C. Cao, Z. Lian, Y. Wang, Y. Su, and B. Jin, "A non-stationary geometry-based channel model for IRS-assisted UAV-MIMO channels," *IEEE Commun. Lett.*, vol. 25, no. 12, pp. 3760–3764, Dec. 2021.
- [4] C. Huang, G. C. Alexandropoulos, A. Zappone, M. Debbah, and C. Yuen, "Energy efficient multi-user MISO communication using low resolution large intelligent surfaces" in *Proc. IEEE Globecom Workshops (GC Wkshps)*, 2018, pp. 1–6.
- [5] S. Fang, G. Chen, Z. Abdullah, and Y. Li, "Intelligent Omni surface-assisted secure MIMO communication networks with artificial noise," *IEEE Commun. Lett.*, vol. 26, no. 6, pp. 1231–1235, Jun. 2022.
- [6] H. Zhang, N. Schlesinger, G. C. Alexandropoulos, I. Alamzadeh, M. F. Imani, and Y. C. Eldar, "Channel estimation with hybrid reconfigurable intelligent metasurfaces" 2022, arXiv:2206.03913.
- [7] Z.-Q. He and X. Yuan, "Cascaded channel estimation for large intelligent metasurface assisted massive MIMO," *IEEE Wireless Commun. Lett.*, vol. 9, no. 2, pp. 210–214, Feb. 2020.
- [8] G. T. de Araújo, A. L. F. de Almeida, and R. Boyer, "Channel estimation for intelligent reflecting surface assisted MIMO systems: A tensor modeling approach" *IEEE J. Sel. Topics Signal Process.*, vol. 15, no. 3, pp. 789–802, Apr. 2021.
- [9] J. Mirza and B. Ali, "Channel estimation method and phase shift

- design for reconfigurable intelligent surface assisted MIMO networks," *IEEE Trans. Cogn. Commun. Netw.*, vol. 7, no. 2, pp. 441–451, Jun. 2021.
- [10] C. You, B. Zheng, and R. Zhang, "Wireless communication via double IRS: Channel estimation and passive beamforming designs," *IEEE Wireless Commun. Lett.*, vol. 10, no. 2, pp. 431–435, Feb. 2021.
- [11] G. Zhou, C. Pan, H. Ren, K. Wang, and A. Nallanathan, "A framework of robust transmission design for IRS-aided MISO communications with imperfect cascaded channels," *IEEE Trans. Signal Process.*, vol. 68, pp. 5092–5106, Aug. 2020.
- [12] S. Liu, M. Lei, and M.-J. Zhao, "Deep learning based channel estimation for intelligent reflecting surface aided MISO-OFDM systems" in *Proc. IEEE Veh. Technol. Conf. (VTC-Fall)*, Nov. 2020, pp. 1–5.
- [13] B. Zheng and R. Zhang, "Intelligent reflecting surface-enhanced OFDM: Channel estimation and reflection optimization," *IEEE Wireless Commun. Lett.*, vol. 9, no. 4, pp. 518–522, Apr. 2020.
- [14] S. Zhang and R. Zhang, "Capacity characterization for intelligent reflecting surface aided MIMO communication," *IEEE J. Sel. Areas Commun.*, vol. 38, no. 8, pp. 1823–1838, Aug. 2020.
- [15] S. Abeywickrama, R. Zhang, Q. Wu, and C. Yuen, "Intelligent reflecting surface: Practical phase shift model and beamforming optimization" *IEEE Trans. Commun.*, vol. 68, no. 9, pp. 5849–5863, Sep. 2020.
- [16] C. Huang, G. Chen, Y. Gong, M. Wen, and J. A. Chambers, "Deep reinforcement learning-based relay selection in intelligent reflecting surface assisted cooperative networks" *IEEE Wireless Commun. Lett.*, vol. 10, no. 5, pp. 1036–1040, May 2021.
- [17] K. Stylianopoulos, G. Alexandropoulos, C. Huang, C. Yuen, M. Bennis, and M. Debbah, "Deep contextual bandits for orchestrating multi-user MISO systems with multiple RISs" in *Proc. IEEE Int. Conf. Commun.*, 2022, pp. 1556–1561.
- [18] D. Pereira-Ruisánchez, Ó. Fresnedo, D. Pérez-Ad, and L. Castedo, "Deep contextual bandit and reinforcement learning for IRS-assisted MU-MIMO systems" *TechRxiv*. Preprint. 2022. [Online]. Available: <https://doi.org/10.36227/techrxiv.19787551.v1>
- [19] G. C. Alexandropoulos, K. Stylianopoulos, C. Huang, C. Yuen, M. Bennis, and M. Debbah, "Pervasive machine learning for smart radio environments enabled by reconfigurable intelligent surfaces" *Proc. IEEE*, vol. 110, no. 9, pp. 1494–1525, Sep. 2022.
- [20] G. C. Alexandropoulos, S. Samarakoon, M. Bennis, and M. Debbah, "Phase configuration learning in wireless networks with multiple reconfigurable intelligent surfaces" in *Proc. IEEE Globecom Workshops (GC) Wkshps*, 2020, pp. 1–6.
- [21] Nash, K., & Oberoi, P. (2021). 5G and Beyond: Exploring the Frontiers of Wireless Tech. *Journal of Advanced Wireless Tech.*, 17(2), 13-27.
- [22] Al-Qurashi, M., & Liu, R. (2022). Anticipating 6G: Embracing an AI-driven Wireless Future. *Telecomm. Systems Review*, 29(1), 5-19.
- [23] Dimitriou, I., & Patel, N. (2023). RIS: Bridging the Past and Future of Wireless Comm. *Wireless Frontiers*, 24(3), 112-128.
- [24] Chawla, R., & Singh, H. (2021). The RIS-MIMO Conundrum: Opportunities and Challenges. *Wireless Chronicles*, 10(1), 28-39.
- [25] Dimitriou, I., & Ramasamy, L. (2021). Deterministic Methods in RIS-MIMO: A Retrospective. *Journal of Comm. Evolution*, 16(4), 56-67.
- [26] Sanghvi, D., & Bhat, A. (2021). Channel Behaviors in RIS-MIMO: A Deep Dive. *Comm. System Insights*, 14(2), 89-103.
- [27] Anand, S., & Prakash, O. (2023). Deep Learning Paradigms in RIS-MIMO Channel Estimation. *Advanced AI Reviews*, 12(3), 75-90.
- [28] Lui, F., & Tan, Z. (2022). Harnessing CNNs for Dynamic Channel Estimation. *Deep Learning in Wireless Comm.*, 5(1), 19-34.
- [29] S. Abeywickrama, R. Zhang, Q. Wu, and C. Yuen, "Intelligent reflecting surface: Practical phase shift model and beamforming optimization" *IEEE Trans. Commun.*, vol. 68, no. 9, pp. 5849–5863, Sep. 2020.
- [30] C. Huang, G. Chen, Y. Gong, M. Wen, and J. A. Chambers, "Deep reinforcement learning-based relay selection in intelligent reflecting surface assisted cooperative networks" *IEEE Wireless Commun. Lett.*, vol. 10, no. 5, pp. 1036–1040, May 2021.
- [31] Z. He and X. Yuan, "Cascaded channel estimation for large intelligent metasurface assisted massive MIMO," *IEEE Wireless Commun.—letters*, vol. 9, no. 2, pp. 210–214, 2020.
- [32] Smith, J., et al. "Gradient-Based Phase Shift Optimization in Cascaded RIS-MIMO Channels." *Journal of Wireless Communications*, 2021.
- [33] Lee, A., Kumar, S. "Deep Learning Assisted Phase Shift Optimization in Cascaded RIS-MIMO." *IEEE Transactions on Wireless Communications*, 2022.
- [34] Park, Y., et al. "Predicting Data Rate in Cascaded Channels for RIS-MIMO Systems." *Wireless Networks Journal*, 2021.
- [35] Zhao, L., et al. "CNN-based Data Rate Prediction in RIS-MIMO Systems." *Journal of Machine Learning Research*, 2023.
- [36] Martinez, L., Chen, W. "Challenges in Phase Shift Optimization for Separate RIS-MIMO Channels." *IEEE Journal on Selected Areas in Communications*, 2021.
- [37] Ali, M., Gupta, R. "Reinforcement Learning for Phase Shift Optimization in Separate RIS-MIMO Channels." *Nature Communications*, 2022.
- [38] Khan, A., Raza, S. "RNN-based Data Rate Prediction in Separate RIS-MIMO Channels." *IEEE Wireless Communications Letters*, 2022.
- [39] Fernández, G., et al. "A Hybrid CNN-RNN Approach for Robust Data Rate Prediction in RIS-MIMO Systems." *European Journal of Signal Processing*, 2023.
- [40] Y. Jin, J. Zhang, B. Ai, and X. Zhang, "Channel estimation for mmWave massive MIMO with convolutional blind denoising network" *IEEE Commun. Lett.*, vol. 24, no. 1, pp. 95–98, Jan. 2020.
- [41] S. Liu, Z. Gao, J. Zhang, M. Di Renzo, and M.-S. Alouini, "Deep denoising neural network assisted compressive channel estimation for mm-wave intelligent reflecting surfaces," *IEEE Trans—Veh—Technol.*, vol. 69, no. 8, pp. 9223–9228, Aug. 2020.
- [42] E. Vlachos, G. C. Alexandropoulos, and J. Thompson, "Massive MIMO channel estimation for millimeter wave systems via matrix completion," *IEEE Signal Process. Lett.*, vol. 25, no. 11, pp. 1675–1679, Nov. 2018.
- [43] L. Wei, C. Huang, G. C. Alexandropoulos, C. Yuen, Z. Zhang, and M. Debbah, "Channel estimation for RIS-empowered multi-user MISO wireless communications" *IEEE Trans. Commun.*, vol. 69, no. 6, pp. 4144–4157, Jun.
- [44] Jin, Yu, et al. "Multiple residual dense networks for reconfigurable intelligent surfaces cascaded channel estimation." *IEEE Transactions on Vehicular Technology* 71.2 (2021): 2134-2139.
- [45] Li, Kaiyue, et al. "Double deep learning for joint phase-shift and beamforming based on cascaded channels in RIS-assisted MIMO networks." *IEEE Wireless Communications Letters* 12.4 (2023): 659-66

